U.Porto Journal of Engineering, 9:3 (2023) 194-208
ISSN 2183-6493
DOI:10.24840/2183-6493_009-003_001749

Received: 5 August, 2022
Accepted: 15 September, 2022
Published: 28 April, 2023

Combustion and Exhaust Emission Improvement in a 3-Cylinder Mpfi Engine Through Downsizing

Sonu Ram[1*], Raj Kumar Yadav[2], Indraj Singh[3]
[1]Mechanical Engineering Department, Sant Longowal Institute of Engineering and Technology, Longowal, Sangrur-148106, Punjab, India, (sonu_pme1807@sliet.ac.in)
[2]Mechanical Engineering Department, Sant Longowal Institute of Engineering and Technology, Longowal, Sangrur-148106, Punjab, India, (rkyd@sliet.ac.in)
[3]Mechanical Engineering Department, Sant Longowal Institute of Engineering and Technology, Longowal, Sangrur-148106, Punjab, India, (indrajsliet@yahoo.co.in)

Abstract

This research aims to compare the potential and existing conditions of a small-sized spark ignition (SI) engine with a 1.0-liter capacity suitable for cylinder deactivation. The cylinder deactivation strategy is used to solve the issues of inefficient combustion and increased exhaust emission under part loading. Consequently, the possibility of implementing cylinder deactivation in terms of decreased exhaust pollution has been assessed. A computerized, 1.0-liter, 4-stroke, water-cooled, spark-ignition engine with an open engine control unit (ECU) and multi-point fuel injection (MPFI) was used for the trials. Both modes were tested at 2500 revolutions per minute (RPM) under loads of 15, 30, and 45 N-m. The spark plug and fuel injector deactivate the cylinder. The results show that when the highest possible load is used, the peak cylinder pressure is 55.78% higher, and the maximum heat release rate is 53.96% more in the deactivation mode than in the traditional mode. In deactivation mode, the mass fraction consumed is larger at each crank angle point, suggesting a faster rate of combustion and increased combustion efficiency. The increased mean gas temperature permits the catalytic converter to perform more efficiently after downsizing. When compared to the conventional mode, carbon monoxide (CO) emission is almost non-existent at full load, unburned hydrocarbon (UHC) is reduced by 92.89%, and oxides of nitrogen (NOx) are reduced by 35% in the deactivation mode. Furthermore, the experiment indicated that, when employed at part load, the deactivation mode is more beneficial than the standard mode in terms of better combustion stability and lesser emissions.

Keywords. Combustion, Cylinder deactivation, Emission, Mpfi, Open ECU

Type: Research Article

1. Introduction

Automotive research should focus on producing an internal combustion (IC) engine with better combustion quality and lesser exhaust emissions for the environment. Currently, it is not possible to eliminate the dependency on fossil fuels in internal combustion engines. However, improving efficiency may reduce fuel consumption, resulting in lower emissions. During an urban driving cycle, an engine's part-load conditions are more than 50% of the time (Flierl et al. 2012; Miklanek et al. 2012). Cylinder deactivation is possible in a spark-ignition engine because part-load circumstances result in less efficient combustion.

According to the literature, half of the cylinders (in 6, 8, and 12-cylinder engines) are cut off using various control systems. Fuel consumption assessment by many researchers has been done under open-throttled conditions using simulation or experimental approaches. There is a scarcity of reports dealing with an evaluation under similar operating conditions for providing the same brake horsepower. Thus, it employed an open engine control unit. This research focuses on the essential engine features of a medium-to-light-duty vehicle, such as combustion and exhaust. This study used a three-cylinder multi-point fuel injection naturally aspirated spark-ignition engine that is often used in Indian operating conditions.

Boretti and Scalco reported that the Cadillac "Modulated Displacement" engine, which operates in V-8-6-4 modes, was initially introduced by General Motors in 1981 (Boretti and Scalco 2011). A deactivated cylinder is chosen based on engine features such as thermal, dynamic, metallurgical, and packaging issues (Bech, Shayler, and McGhee 2016). At part load, the turbocharged spark ignition and 4-cylinder compression ignition engines reduce exhaust emissions. However, the advantages are lower when the more dynamic ARTEMIS (Assessment and Reliability of Transport Emission) cycle is utilized (El Shenawy et al. 2019; Feng et al. 2013). According to an analytical and experimental examination, when a 6-cylinder engine was operated in 3-cylinder mode, exhaust emissions were within allowable limits for the same torque-producing situation (Elfasakhany and Mahrous 2016). Downsizing a direct injection SI engine with compressed natural gas (CNG) outperforms gasoline in exhaust emissions (Nanthagopal et al. 2018). Maintaining higher exhaust temperatures while deactivating cylinders improves the performance of diesel particulate filters (Mashadi and Maleki 2014; McGhee et al. 2019). Cylinder deactivation results in a thinner lubricating coating, leading to increased frictional power losses. In working cylinders due to the higher pressure combustion gas leakage increases (Orjuela Abril, Fonseca-Vigoya, and García 2022). Brake-specific fuel consumption has been improved by up to 30 percent, while engine emissions have an insignificant effect (Thamotharan, Naveenchandran, and Raja 2022). Ben knight reported that as the number of cylinders increases the cost of minimizing noise and vibration also enhanced for the application of cylinder deactivation. Implementation of cylinder deactivation for large-capacity gasoline engines would cost between $203 and $229 (Knight 2010). Despite this additional cost, about power availability and comfort noise, vibration, and harshness (NVH) attributes have equal metrics (Faust and Scheidt 2016). This article illustrates that deactivation mode results in the cost of vibration and power loss while operating at a fully open throttle valve (Parker et al. 2021). The main advantage of MPFI engines is that it prevents emitting particulates caused by generating a well premixed and almost homogenous charge inside the combustion chamber, resulting in a stoichiometric mixture. As a result, the combustion chamber has no fuel-air-rich mixture zones, and soot production is negligible (Barboza, Mohan, and Dinesha 2022).

The problem for the Indian vehicle industry is meeting government pollution limits while still meeting customer demand. This study area appears to have gotten less attention, so there is still room for improvement in exhaust emissions for SI engines. The cylinder deactivation approach may be the best alternative for researching its impact on combustion and exhaust pollution. Because three-cylinder engines are the most common in India, this study emphasizes that.

2. Materials and Methods

2.1. Test Rig and Equipment

This experiment was carried out on a naturally aspirated MPFI SI engine having a capacity of 998 cubic centimeters and three cylinders. An open ECU is included in this test setup. An eddy current dynamometer was mounted to impart a load to the engine. Engine speed and other sensor data are gathered using a data acquisition system saved on a personal computer. In **Table 1**, the engine specifications are listed. A test rig is depicted schematically in **Figure 1**. The characteristics of measuring equipment and sensors are shown in **Table 2**. Emissions were measured using an AVL-444 exhaust gas analyzer.

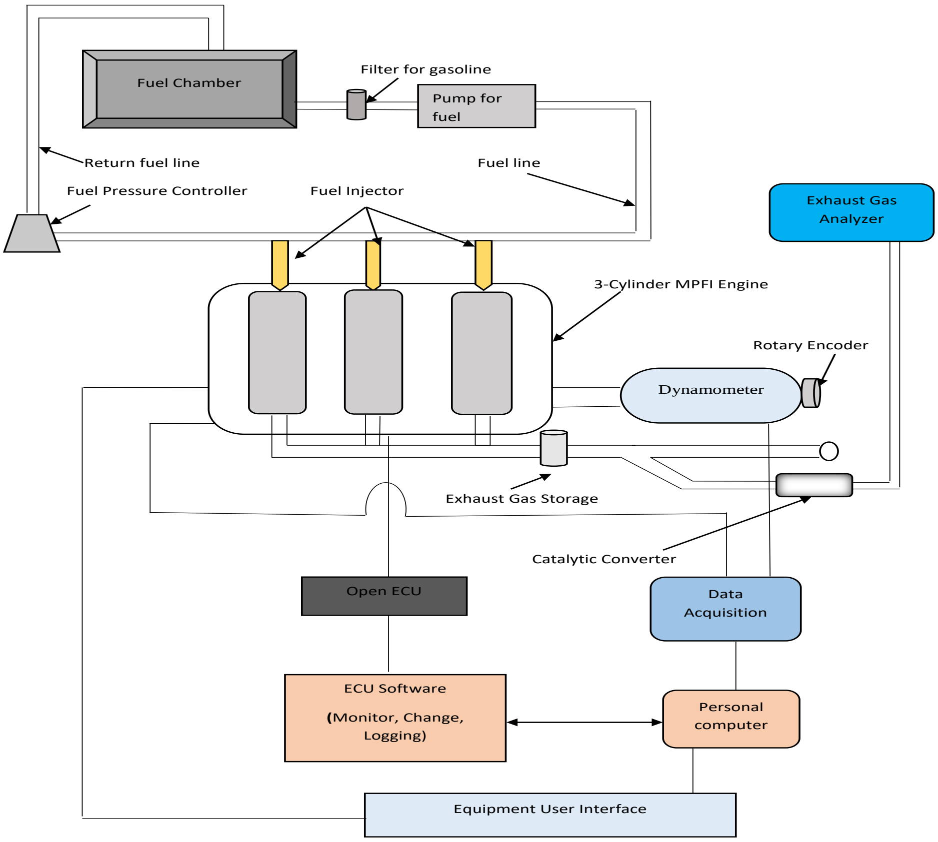

Figure 1: An experimental setup's schematic

Number of Cylinders	3 (Three)
Ignition by	Spark Plug
Fuel Injection	Multi-point fuel injection
Strokes Count	4
Engine Manufacturer	Maruti Suzuki India Limited
Engine Capacity (Displacement)	998 Cc (Cubic Centimetre)
Engine shaft revolution per minute	1000-5500
Maximum Load Condition	60 Nm load at 3500 revolution/minute
Engine Control Unit	Open Type
Exhaust Emission Standard	Bharat Stage-IV
Total Volume/Clearance Volume	9.5:1
Length of Stroke (mm)	79.5
Diameter of Bore (mm)	72
Maximum Brake Horse Power	50 hp at 5000 revolution/minute
Valve count per Cylinder	Four

Table 1. Specification of the 3-cylinder engine

Measuring Instruments/Sensor	Specification/Make/Location
Water Cooled Eddy Current Dynamometer	Strain Gauge Type Load Cell, Technomac Tme-100
Combustion Pressure Sensor	Pcb 113a22 /In The Cylinder Head
Crank Angle Measurement	Rotary Encoder/ Autonics E50s8
Solenoid Valve	Uflow Dan14z
Intake Air Flow Measurement	Bosch Hfm-5
Data Acquisition Software	Engine Scan Is A Ni LabVIEW Based
Fuel Pressure Transmitter	Dawyer 628 Series, Piezoresistive Transmitter
Engine Control Unit	Nira Control AB, Sweden, MCS1
Cam Position Sensor	Maruti Suzuki
Crank Position Sensor	Bosch, Dg6
Exhaust Temp. Sensor	Sensata Technologies Inc., Darts200-Aw
Gasoline Injector	Denso/Maruti Suzuki, Saturated Type
Exhaust Gas Analyser	AVL 444 DIGAS

Table 2. Measurement instrument/sensor specification

2.2. Method of Experiment

This experimental research features two operating modes: conventional mode (CM), where all three cylinders are operational, and cylinder deactivation mode (CDM), where one cylinder is inactive. After conducting a pilot experiment, it was determined that the engine could absorb up to 45 Nm of load by deactivating one cylinder. The present investigation uses a 2500 rpm speed of an engine and a variable load of 15, 30, and 45 Nm. Because the engine operates under the same load and speed input circumstances, the comparison is based on delivering the same brake horsepower (BHP) in both modes. Engine combustion and emissions are monitored based on the inputs supplied for each experiment, as indicated in **Table 3**. An average of 10 cycles was used to reduce experimental error. Based on the load and speed input, the open ECU updates the other operating parameters mentioned in **Table 4**. Turn on the load/unload button on the equipment user interface (EUI) front panel under the load control section to activate the load controller. To get a precise load value, the potentiometer should be gradually adjusted. The engine receives direct load through the built-in load controller, and the load value obtained by the load cell is presented in the data-gathering application Engsoft1.0. The open ECU software displays the accelerator pedal position and the engine RPM.

Load (N-m)	Engine Response Parameters	
	Combustion	Emissions
15 30 45	Cylinder pressure (CP) Heat release rate (HRR) Mass fraction burned (MFB) Mean gas temperature (MGT)	Carbon monoxide (CO) Carbon dioxide (CO_2) Unburned hydrocarbon (UHC) Oxides of nitrogen (NO_x)

Table 3. Engine testing at 2500 RPM with conventional and cylinder deactivation mode

Speed (RPM)	Load (N-m)	Throttle Opening (%)		Fuel Injection Time (bTDC)		Spark Time (bTDC)	
		CM	CDM	CM	CDM	CM	CDM
2500	15	10.2	12.7	220	220	20	20
2500	30	11.8	17	220	220	20	20.2
2500	45	14.8	32.6	220	227	20	20.7

Table 4. Engine operating condition for same brake horsepower generation in CM and CDM

3. Results and Discussion

3.1. Combustion Analysis

A plot of combustion properties is shown in **Figures 2-8**. The maximum value of all these parameters is represented using a bar graph at 2500 rpm for all loading situations. However, for the best findings, the variance of each parameter was also examined about crank angle position. The top dead center (TDC) position is denoted by zero degrees. **Table 5** shows the engine operating conditions for combustion analysis, including input and response parameters.

LOAD (N-m)	Peak Pressure (bar)		Maximum HRR (J)		MGT (^{0}C)	
	CM	CDM	CM	CDM	CM	CDM
15	11.05	21.99	8.80	17.51	977.41	1360.18
30	20.33	34.02	15.48	26.60	1268.01	1815.20
45	29.56	46.05	23.24	35.78	1640.51	2288.35

Table 5. Engine combustion parameters at 2500 RPM for CM and CDM

3.1.1. Cylinder Pressure

Figure 2 depicts a load-peak pressure curve. Peak pressure increases as the load on the engine rise because more charge must be burned to maintain the power output. **Figure 3** shows how cylinder pressure varies with the crank angle in CDM and CM. When the engine is switched from conventional to deactivation mode, the variation of the cylinder pressure is greatly influenced. In deactivation mode, the cylinder pressure is higher than in CM when the piston is near TDC. In the CM, the maximal cylinder pressure is 29.56 bar at 21^o CA after TDC, and in CDM is 46.05 bar at 18^o CA after TDC, indicating that in CDM, the peak location has been shifted closer to TDC. A 55.78 % rise in peak pressure is found during CDM compared to CM due to the accessible rich mixture, resulting in improved diffusion stage combustion (Singh et al. 2020). The ignition timing for CM is 20^0 CA before TDC, and in CDM is 20.7^0 CA before TDC; therefore, in CDM, the charge ignites earlier, reducing the dissipation of heat, increasing the expansion proportion, and improving the combustion of fuel. It has been discovered that in CDM, early ignition occurs, as presented in **Table 4**, which may increase cylinder pressure to retain the same power and improve combustion efficiency (Zhang et al. 2021). The trend is identical for both modes, albeit the highest load handled by the engine during CDM is 45 N-m.

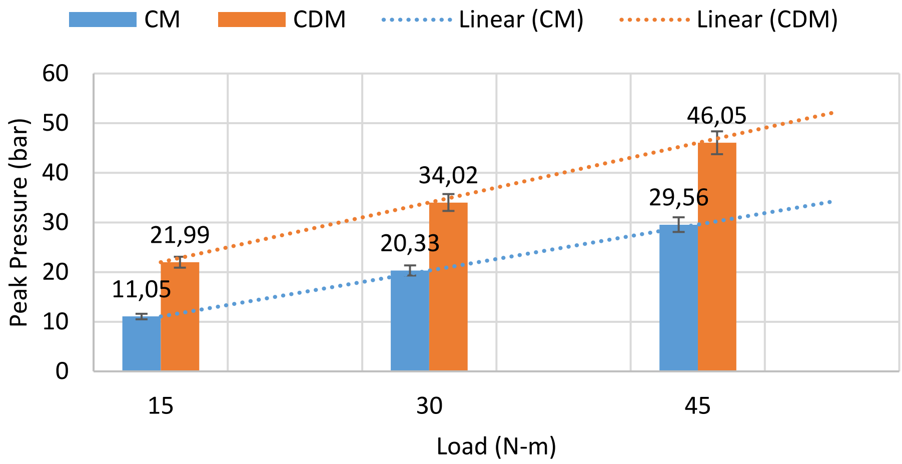

Figure 2: Variation in peak pressure versus engine load

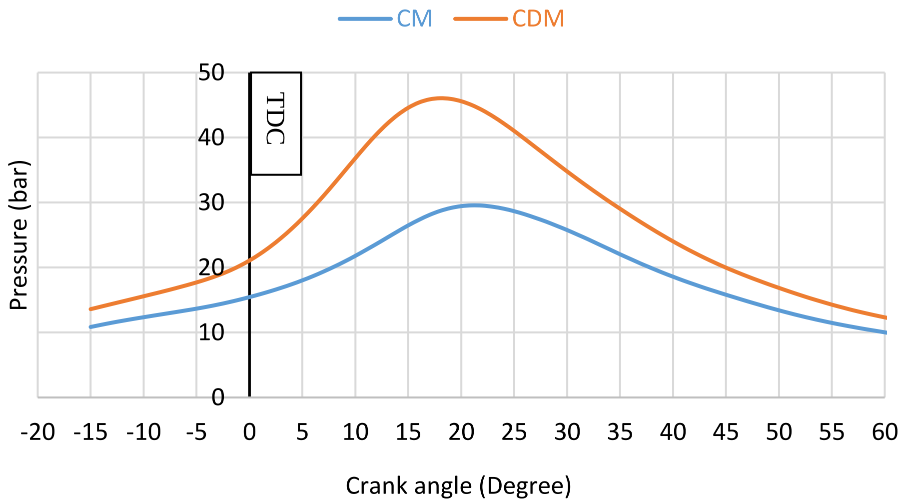

Figure 3: Change in-cylinder pressure versus crank position at full load

3.1.2. Heat Release Rate

Figure 4 depicts the fluctuation of maximum HRR with engine load. There is no change in the load between the two modes; however, only two cylinders are engaged in CDM, compared to all three cylinders in CM. Therefore, the engine operates at full load during deactivation mode. As a result, the throttle is opened wider, meaning that a rich fuel mixture encourages high pressure and temperature, both of which are desirable for increased HRR in CDM (Yaman and Yesilyurt 2021). **Figure 5** shows how the crank angle affects the rate of heat emission for the CM and CDM. The maximum heat release rate in CM is 23.24 J/deg at 16^0 CA after TDC, and in CDM is 35.78 J/deg at 12^0 CA after TDC. It has been discovered that when a cylinder is deactivated due to advanced spark ignition timing compared to CM, which aids early and quick ignition of charge to promote combustion at greater engine loads, the apex of HRR shifts closer to TDC. Another explanation for the variation in HRR across modes is that the spark ignition timing in CDM is advanced. Factors influencing HRR include the MPFI SI engine's efficient charge mixing, combustion rate, and calorific value (Sivasubramanian et al. 2017). In the CDM, more overall heat is emitted than in the CM, with most of it discharged after TDC.

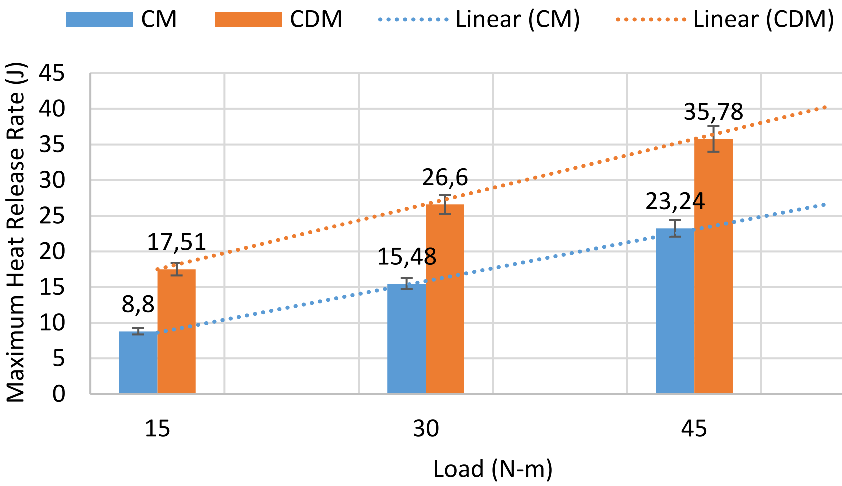

Figure 4: Variation in Maximum HRR Versus Engine Load

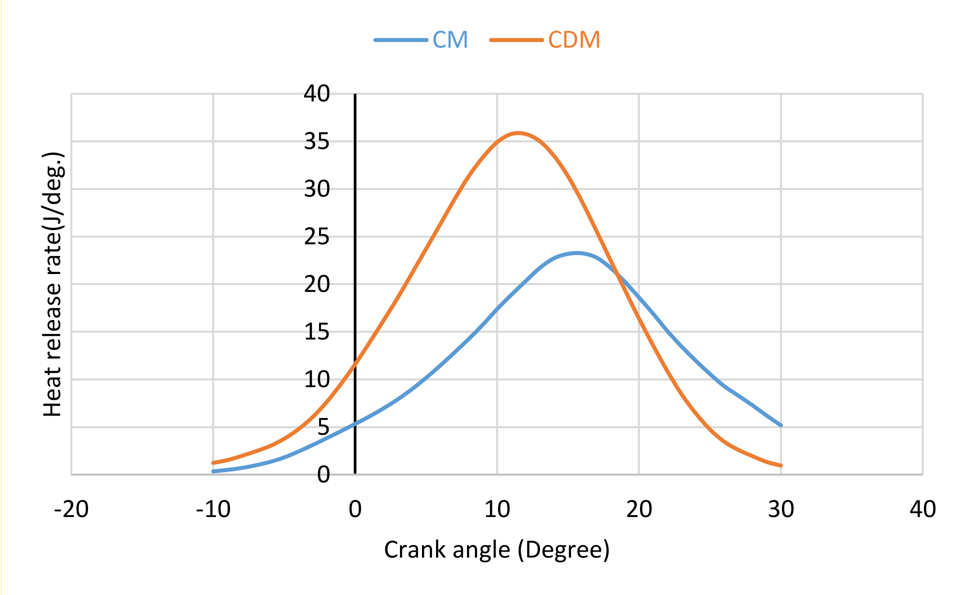

Figure 5: HRR variation with a crank angle when fully loaded

3.1.3. Mass Fraction Burned

Figure 6 demonstrates how MFB varies with the crank angle in CM and CDM. MFB usually has a relationship between the rate of combustion inside the engine and the crank angle. In a sequential combustion process, the proportion of emitted heat to overall heat is defined as MFB. It depends on various parameters such as engine running state, engine type, and combustion quality. In the case of deactivation mode, it was discovered that a lower A/F ratio and a 0.7^0 CA advanced ignition angle play a critical role in obtaining greater MFB for the same loading situation and engine speed. As a result, in deactivation mode, energy conversion is more significant than in regular mode. The length of the combustion process is also observed to be shorter in the deactivation mode. Researchers study MFB in two phases, with up to 10% of mass burning occurring in the first phase and 10% to 90% of the second. This mass burning is related to crank angle and is recorded as a combustion rate (Zhang et al. 2014; Wang et al. 2013; Agarwal, Karare, and Dhar 2014; Gong et al. 2016). As seen in **Figure 6**, the combustion rate in CDM is faster than in CM.

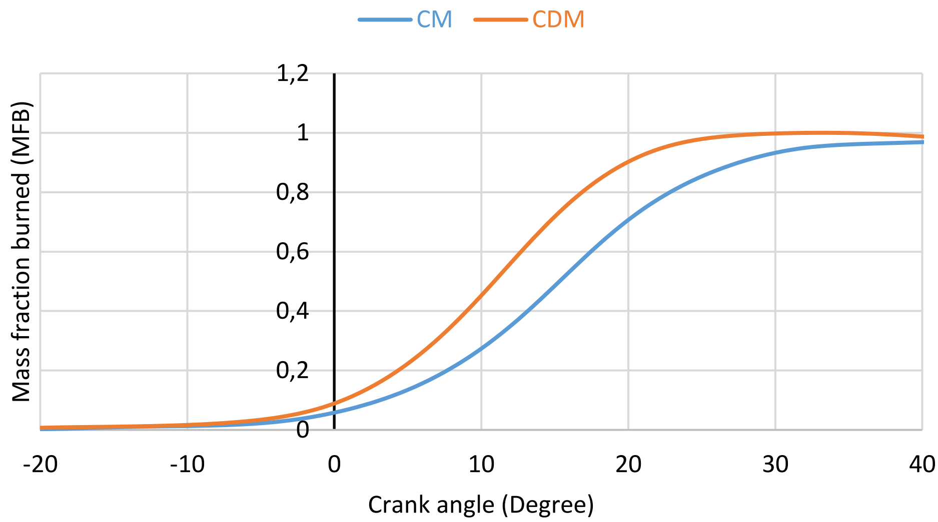

Figure 6: Change in MFB with the crank angle at full load

3.1.4. Mean Gas Temperature

A plot between MGT and engine load has been shown in **Figure 7**. It is found that as the load on the engine increases due to more energy requirements, higher fuel is burned; thus, MGT increases. **Figure 8** depicts the fluctuation of mean gas temperature with the crank angle in CM and CDM. MGT is greater in CDM because the engine operates at a higher load than CM, leading to a broader throttle opening. Consequently, a rich mixture intake and a more significant heat release than CM (Zhang et al. 2021). Another possible reason for higher MGT in CDM is that the lower A/F ratio encourages more heat absorption by nitrogen. The last portions of CDM state that when load increases on the operating cylinder, the flame duration will be shortened, and there would be a larger MGT than there would be under CM (Ramesh Kumar and Nagarajan 2012).

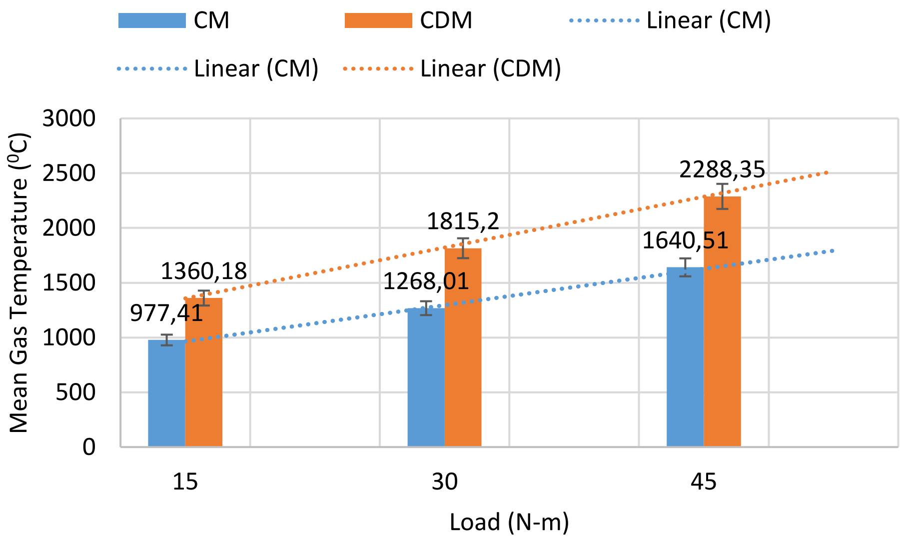

Figure 7: Variation in mean gas temperature versus engine load

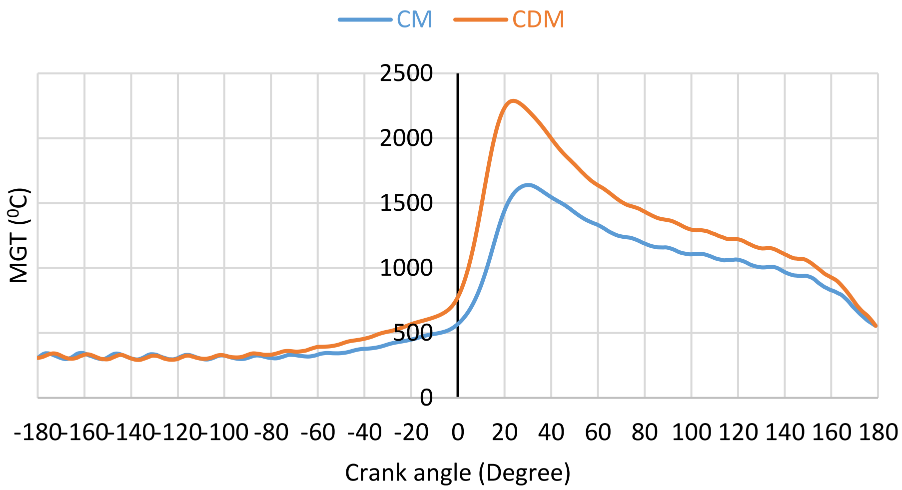

Figure 8: MGT variation with the crank position under full load

3.2. Emission Analysis

The emission characteristics results are classified into four output parameters: CO, CO_2, UHC, and NO_X. To assess emissions in raw concentrations of percent volume and ppm, an exhaust gas analyzer (AVL 444) was employed. Results for exhaust emission in both modes are shown in Table 6 for three engine loads at a speed of 2500 RPM.

		Conventional Mode				Cylinder Deactivation Mode			
Speed (RPM)	Load (N-m)	CO	CO_2	UHC	NO_x	CO	CO_2	UHC	NO_x
2500	15	0.85	12.90	244	52	0.00	10.30	36	395
	30	4.06	10.80	349	61	0.01	8.90	33	189
	45	5.21	9.50	394	140	0.01	11.70	28	91

Table 6. Exhaust emission data for CM and CDM

3.2.1 Carbon Monoxide

The restricted emission regulations should regulate it since carbon monoxide is a dangerous poisonous gas. **Figure 9** depicts how CO emissions from both combustion modes rise as the engine approaches its load limit. As we know, CO is intimately connected to the fuel-air proportion and comes from incomplete fuel combustion. Cylinder deactivation can lower CO emissions dramatically by increasing the charge mass inside the cylinder resulting in a better state of combustion owing to a more significant throttle opening. Because of the entire burning process caused by the increased load on the engine, the rich mixture intake follows; thus, CO trends revealed that regular mode combustion emitted much more CO than deactivation mode combustion. The fundamental explanation for this tendency is the relatively higher in-cylinder temperature. This was most likely because the temperature within the cylinder had increased, which directly impacted the oxidation of CO to CO_2. Higher combustion temperatures raise the exhaust gases' temperatures, enhancing the mixture's swirling and oxidation (Wang, Ji, and Zhang 2010; Parker et al. 2021; Zammit et al. 2014).

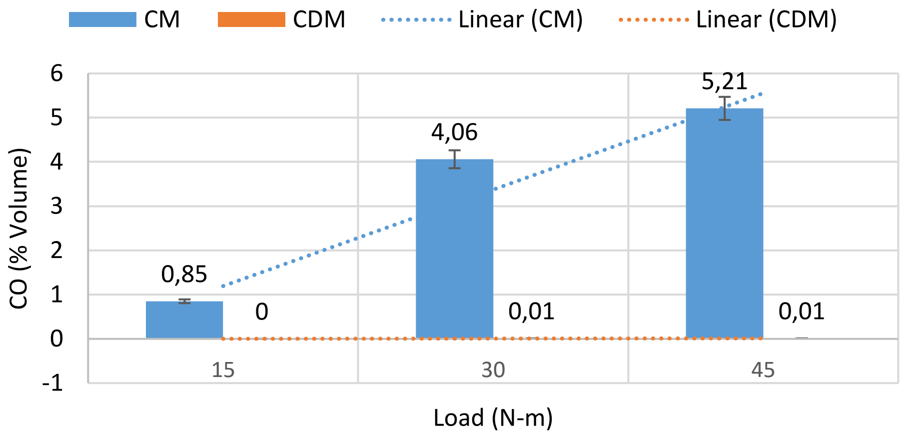

Figure 9: Emission of CO versus engine load for both the modes

It is found that fresh air from deactivated cylinders combines with exhaust gas facilitating carbon monoxide oxidation to carbon dioxide. (Singh and Sahni 2017) revealed that greater oxygen concentration helps to improve the fuel's ability to burn completely. Across the spectrum of engine loads, reduced CO engine-out emissions were found. Increased cylinder pressure causes micro-explosion, which is generated by a greater chamber temperature and intensifies carbon oxidation by oxygen in chemical reactions. It was discovered that at greater engine loads, a significant increase of MGT diminished the benefits of early spark ignition resulting in nearly identical CO emissions in deactivation modes under all spectrums of loads. MGT would be lower under low loading situations, as is widely established. To summarise, a lower combustion temperature reduces CO_2 emissions. However, when more loading circumstances arose, fuel usage rose, and a short combustion time resulted in higher CO emission generation.

3.2.2 Carbon Dioxide

In a SI engine, CO_2 in the exhaust gases confirms that fuel has been completely burned. CO_2 emissions fall when the load increases from 15 N-m to 45 N-m in normal mode, but in deactivation, it reduces and then increases, as illustrated in **Figure 10**. CO_2 emissions are lesser during CDM than in the CM up to a 30 N-m load and higher at 45 N-m loads owing to better combustion and lower oxygen availability than in the normal mode. Under a load of 45 N-m and 2500 RPM, CO_2 emissions are reduced due to higher combustion efficiency. However, this load acts as a full engine load during CDM, so the throttle is wide open, and the engine works on a greater fuel and air mixture resulting in more oxygen availability and a higher temperature favorable for CO_2 emission at this point. It has been discovered that air from deactivated cylinders discharges into the exhaust, converting CO into CO_2. CO_2 emissions are reduced in GDI, although DI CNG is more advantageous in deactivation mode (Kar et al. 2021). Furthermore, CO_2 emissions impact the effectiveness of the engine combustion process. It is claimed and discovered regarding the engine's combustion process that it was more effective when higher CO_2 emissions were released (Feng et al. 2013). It was found that CO_2 emissions were typically affected by the air-fuel ratio, the quantity of CO, and UHC emissions (Yaman and Yesilyurt 2021).

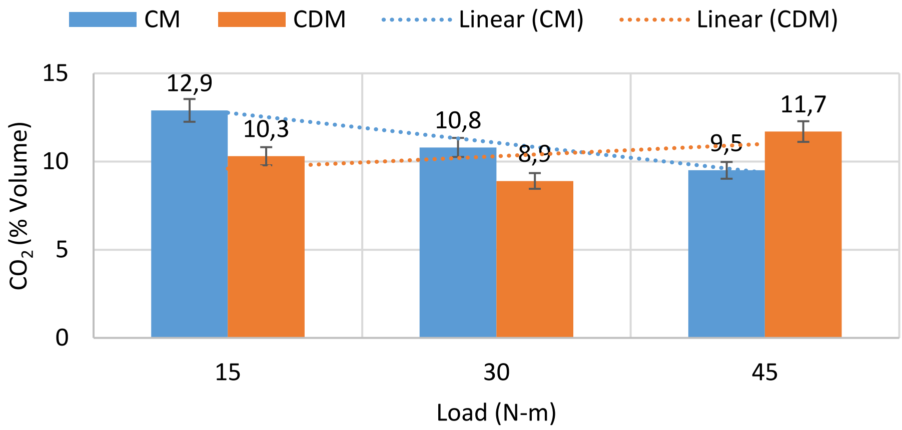

Figure 10: Emission of CO_2 versus engine load for both modes

3.2.3 Unburned Hydrocarbon

The principal cause of unburned hydrocarbon emissions in an engine is incomplete combustion. It is determined by the A/F ratio, load, speed, and mode of operation. As seen in **Figure 11**, in CM, as the load on the engine grows, so does UHC due to incomplete combustion at part loading. This is primarily due to incomplete combustion due to a lower air-fuel ratio, but in deactivation mode, as the load increases, the engine tends towards full loading, so the UHC trend is the opposite, indicating higher combustion efficiency and decreased emissions of UHC over the spectrum of engine loads. Higher MGT encourages a faster rate of oxidation and perhaps enhanced dissipation of gasoline from the moist surfaces resulting in continuous reductions in UHC emissions. Because there is more load in deactivation mode, there is a broader opening of the throttle and a richer mixture than in normal mode resulting in higher temperature and pressure favorable for improved fuel combustion. UHC emissions were lowered across the board due to improved combustion efficiency. By using cylinder deactivation technology, the quantity of unburned fuel that enters the piston crevices due to gas blow-by is minimized (Orjuela Abril, Fonseca-Vigoya, and García 2022).

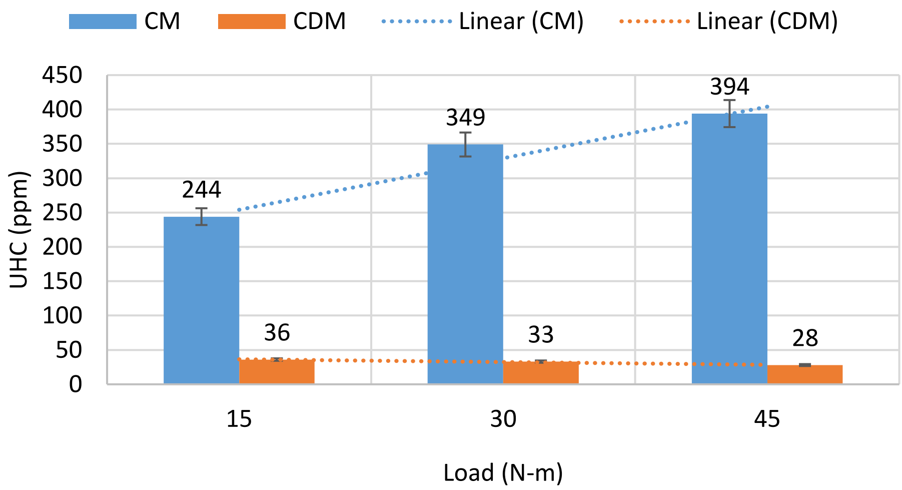

Figure 11: Emission of UHC versus engine load for both modes

3.2.4 Oxides of Nitrogen (NO_x)

The major causes of NOx emissions are increased temperature and oxygen availability. As demonstrated in **Figure 12**, CM load increases, promoting the high-temperature dissociation processes that contribute to NOx formation, whereas this tendency is reversed in deactivation mode. The temperature of a traditional SI engine rises as the load rises, and the engine operates on a rich mixture resulting in the highest NOx emissions (Kar et al. 2021). In deactivation mode, the active cylinder operates at a greater load because the load of the deactivated cylinder is moved to the active cylinder as opposed to the CM. This leads to rich mixture burning, which creates a higher temperature and pressure favorable for NOx generation. It has been discovered that at 45 N-m loads, NOx emission in the CDM is lesser than in the CM. The fact that the light-off temperature has been achieved, which increases the effectiveness of the catalytic converter, might be the cause of this development due to lower NOx emissions. Tailpipe NOx reductions can be achieved via cylinder deactivation and after-treatment thermal management. However, in deactivation mode, free oxygen is available from the deactivated cylinder when it mixes with flue gases more air than stoichiometric, promoting a reduction in peak temperature and less NOx emission (Turnbull et al. 2021).

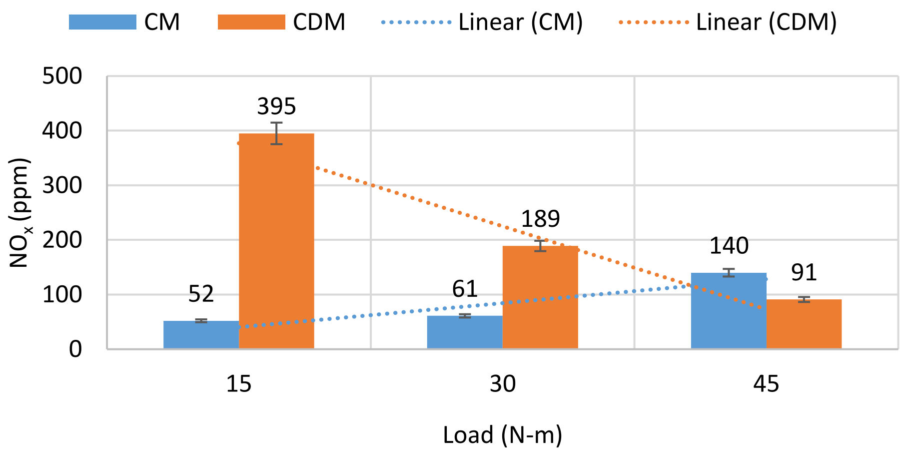

Figure 12: Emission of NO_x versus engine load for both modes

4. Conclusions

This experimental research investigated the evaluation of combustion and emission parameters under identical operating conditions for producing the same braking horsepower with and without cylinder deactivation mode. The following findings have been formed based on observations: -

1. Peak pressure rose by 55.78% in deactivation mode compared to CM. After the compression stroke has finished, the peak cylinder pressure in CDM is discovered early. The more rapid and effective combustion is indicated. Despite this, testing has also shown that the deactivation mode results in a higher noise and vibration level.
2. Higher HRR and a peak that is close to TDC in deactivation mode imply improved combustion, which effectively converts heat into work.
3. Better combustion efficiency and a quicker burning rate correlate with higher MFB. As a result, more excellent energy conversion in deactivation mode compared to CM.
4. Deactivation mode produces greater mean gas temperatures than CM because the engine operates at full load and experiences increased swirl, turbulence, and F/A ratio.

This temperature rise allows the catalytic converter to operate more effectively in deactivation mode.

5. In CDM, CO emissions from the tailpipe are negligible at all loading levels. However, CO2 emissions are reduced up to 35 N-m and greater at maximum load. The temperature in the cylinder increases due to the gasoline being completely used up, allowing CO to be converted to CO2.
6. Compared to CM, the amount of UHC in the deactivation mode is reduced by 92.89% at the maximum load. Higher combustion efficiency and full load operation of still active cylinders are the driving forces behind this advancement.
7. In CDM, when the load is increased, NOx emissions decrease, with the lowest value seen on the higher loading side. The in-cylinder temperature is higher, and mixing fresh air from the deactivated cylinder results in a drop in exhaust gas temperature, which makes the catalytic converter perform more effectively and reduces NOx emissions by 35%.

References

Agarwal, Avinash Kumar, Himanshu Karare, and Atul Dhar. 2014. “Combustion, Performance, Emissions and Particulate Characterization of a Methanol–Gasoline Blend (Gasohol) Fuelled Medium Duty Spark Ignition Transportation Engine.” Fuel Processing Technology 121 (May): 16–24. https://doi.org/10.1016/j.fuproc.2013.12.014.

Barboza, Augustine B.V., Sooraj Mohan, and P. Dinesha. 2022. “Influence of Hydrogen Peroxide Emulsification with Gasoline on the Emissions and Performance in an MPFI Engine.” International Journal of Hydrogen Energy 47 (59): 25034–43. https://doi.org/10.1016/j.ijhydene.2022.05.229.

Bech, Alexander, Paul J. Shayler, and Michael McGhee. 2016. “The Effects of Cylinder Deactivation on the Thermal Behaviour and Performance of a Three Cylinder Spark Ignition Engine.” SAE International Journal of Engines 9 (4): 1999–2009. https://doi.org/10.4271/2016-01-2160.

Boretti, Alberto, and Joseph Scalco. 2011. “Piston and Valve Deactivation for Improved Part Load Performances of Internal Combustion Engines.” In , 2011-01–0368. https://doi.org/10.4271/2011-01-0368.

El Shenawy, E.A., Medhat Elkelawy, Hager Alm-Eldin Bastawissi, Mahmoud M. Shams, Hitesh Panchal, Kishorkumar Sadasivuni, and Nishant Thakar. 2019. “Investigation and Performance Analysis of Water-Diesel Emulsion for Improvement of Performance and Emission Characteristics of Partially Premixed Charge Compression Ignition (PPCCI) Diesel Engines.” Sustainable Energy Technologies and Assessments 36 (December): 100546. https://doi.org/10.1016/j.seta.2019.100546.

Elfasakhany, Ashraf, and Abdel-Fattah Mahrous. 2016. “Performance and Emissions Assessment of N-Butanol–Methanol–Gasoline Blends as a Fuel in Spark-Ignition Engines.” Alexandria Engineering Journal 55 (3): 3015–24. https://doi.org/10.1016/j.aej.2016.05.016.

Faust, Hartmut, and Martin Scheidt. 2016. “Cylinder Deactivation — Potentials & Constraints.” Auto Tech Review 5 (10): 38–43. https://doi.org/10.1365/s40112-016-1218-4.

Feng, Renhua, Jing Yang, Daming Zhang, Banglin Deng, Jianqin Fu, Jingping Liu, and Xiaoqiang Liu. 2013. “Experimental Study on SI Engine Fuelled with Butanol–Gasoline Blend and H2O Addition.” Energy Conversion and Management 74 (October): 192–200. https://doi.org/10.1016/j.enconman.2013.05.021.

Flierl, Rudolf, Frederic Lauer, Michael Breuer, and Wilhelm Hannibal. 2012. “Cylinder Deactivation with Mechanically Fully Variable Valve Train.” SAE International Journal of Engines 5 (2): 207–15. https://doi.org/10.4271/2012-01-0160.

Gong, Changming, Fenghua Liu, Jingzhen Sun, and Kang Wang. 2016. “Effect of Compression Ratio on Performance and Emissions of a Stratified-Charge DISI (Direct Injection Spark Ignition) Methanol Engine.” Energy 96 (February): 166–75. https://doi.org/10.1016/j.energy.2015.12.062.

Kar, Tanmay, Zhenbiao Zhou, Michael Brear, Yi Yang, Maziar Khosravi, and Joshua Lacey. 2021. “A Comparative Study of Directly Injected, Spark Ignition Engine Performance and Emissions with Natural Gas, Gasoline and Charge Dilution.” Fuel 304 (November): 121438. https://doi.org/10.1016/j.fuel.2021.121438.

Knight, Ben. 2010. “Better Mileage Now.” Scientific American 302 (2): 50–55. https://doi.org/10.1038/scientificamerican0210-50.

Mashadi, B., and A. Maleki. 2014. "Influence of cylinder deactivation technology on fuel consumption and emissions of four-cylinder spark ignition engine." The Journal of Engine Research 35 (35): 41-51.

McGhee, Michael, Ziman Wang, Alexander Bech, Paul J Shayler, and Dennis Witt. 2019. “The Effects of Cylinder Deactivation on the Thermal Behaviour and Fuel Economy of a Three-Cylinder Direct Injection Spark Ignition Gasoline Engine.” Proceedings of the Institution of Mechanical Engineers, Part D: Journal of Automobile Engineering 233 (11): 2838–49. https://doi.org/10.1177/0954407018806744.

Miklanek, Lubomir, Oldrich Vitek, Ondrej Gotfryd, and Vojtech Klir. 2012. “Study of Unconventional Cycles (Atkinson and Miller) with Mixture Heating as a Means for the Fuel Economy Improvement of a Throttled SI Engine at Part Load.” SAE International Journal of Engines 5 (4): 1624–36. https://doi.org/10.4271/2012-01-1678.

Nanthagopal, K., B. Ashok, B. Saravanan, Deepam Patel, B. Sudarshan, and R. Aaditya Ramasamy. 2018. “An Assessment on the Effects of 1-Pentanol and 1-Butanol as Additives with Calophyllum Inophyllum Biodiesel.” Energy Conversion and Management 158 (February): 70–80. https://doi.org/10.1016/j.enconman.2017.12.048.

Orjuela Abril, Sofia, Marlen Del Socorro Fonseca-Vigoya, and Carlos Pardo García. 2022. “Study of the Cylinder Deactivation on Tribological Parameters and Emissions in an Internal Combustion Engine.” Lubricants 10 (4): 60. https://doi.org/10.3390/lubricants10040060.

Parker, Matthew C, Changzhao Jiang, Daniel Butcher, Adrian Spencer, Colin P Garner, and Dennis Witt. 2021. “Impact and Observations of Cylinder Deactivation and Reactivation in a Downsized Gasoline Turbocharged Direct Injection Engine.” International Journal of Engine Research 22 (4): 1367–76. https://doi.org/10.1177/1468087419882817.

Ramesh Kumar, C., and G. Nagarajan. 2012. “Performance and Emission Characteristics of a Low Heat Rejection Spark Ignited Engine Fuelled with E20.” Journal of Mechanical Science and Technology 26 (4): 1241–50. https://doi.org/10.1007/s12206-012-0206-0.

Singh, Akhilendra Pratap, Vikram Kumar, and Avinash Kumar Agarwal. 2020. “Evaluation of Comparative Engine Combustion, Performance and Emission Characteristics of Low Temperature Combustion (PCCI and RCCI) Modes.” Applied Energy 278 (November): 115644. https://doi.org/10.1016/j.apenergy.2020.115644.

Singh, Indraj, and V Sahni. 2017. “Impact of Emission on Environment of Electric Generator Fuelled with Karanja (Pongamia Pinnata) Biodiesel Adding Additive Di-Ethyl Ether.” Nature

Environment and Pollution Technology 16 (3): 861–66. https://neptjournal.com/upload-images/NL-61-26-(24)B-3438.pdf.

Sivasubramanian, Harish, Yashwanth Kutti Pochareddy, Gopinath Dhamodaran, and Ganapathy Sundaram Esakkimuthu. 2017. "Performance, Emission and Combustion Characteristics of a Branched Higher Mass, C 3 Alcohol (Isopropanol) Blends Fuelled Medium Duty MPFI SI Engine." Engineering Science and Technology, an International Journal 20 (2): 528–35. https://doi.org/10.1016/j.jestch.2016.11.013.

Turnbull, Robert, Nader Dolatabadi, Ramin Rahmani, and Homer Rahnejat. 2021. "Energy Loss and Emissions of Engine Compression Rings with Cylinder Deactivation." Proceedings of the Institution of Mechanical Engineers, Part D: Journal of Automobile Engineering 235 (7): 1930–43. https://doi.org/10.1177/0954407020982868.

Vinod kumar, Mn, C. Thamotharan, P. Naveenchandran, and E. Raja. 2022. "Cylinder Deactivation Technique in Multi-Cylinder Engines for Fuel Consumption Reduction." Journal of Physics: Conference Series 2272 (1): 012028. https://doi.org/10.1088/1742-6596/2272/1/012028.

Wang, Chongming, Hongming Xu, Ritchie Daniel, Akbar Ghafourian, Jose Martin Herreros, Shijin Shuai, and Xiao Ma. 2013. "Combustion Characteristics and Emissions of 2-Methylfuran Compared to 2,5-Dimethylfuran, Gasoline and Ethanol in a DISI Engine." Fuel 103 (January): 200–211. https://doi.org/10.1016/j.fuel.2012.05.043.

Wang, Shuofeng, Changwei Ji, and Bo Zhang. 2010. "Effects of Hydrogen Addition and Cylinder Cutoff on Combustion and Emissions Performance of a Spark-Ignited Gasoline Engine under a Low Operating Condition." Energy 35 (12): 4754–60. https://doi.org/10.1016/j.energy.2010.09.015.

Yaman, Hayri, and Murat Kadir Yesilyurt. 2021. "The Influence of N-Pentanol Blending with Gasoline on Performance, Combustion, and Emission Behaviors of an SI Engine." Engineering Science and Technology, an International Journal 24 (6): 1329–46. https://doi.org/10.1016/j.jestch.2021.03.009.

Zammit, Jean-Paul, Michael J McGhee, Paul J Shayler, and Ian Pegg. 2014. "The Influence of Cylinder Deactivation on the Emissions and Fuel Economy of a Four-Cylinder Direct-Injection Diesel Engine." Proceedings of the Institution of Mechanical Engineers, Part D: Journal of Automobile Engineering 228 (2): 206–17. https://doi.org/10.1177/0954407013506182.

Zhang, Peng, Jimin Ni, Xiuyong Shi, Sheng Yin, and Dezheng Zhang. 2021. "Effects of Ignition Timing on Combustion Characteristics of a Gasoline Direct Injection Engine with Added Compressed Natural Gas under Partial Load Conditions." Processes 9 (5): 755. https://doi.org/10.3390/pr9050755.

Zhang, Zhijin, Tianyou Wang, Ming Jia, Qun Wei, Xiangzan Meng, and Gequn Shu. 2014. "Combustion and Particle Number Emissions of a Direct Injection Spark Ignition Engine Operating on Ethanol/Gasoline and n-Butanol/Gasoline Blends with Exhaust Gas Recirculation." Fuel 130 (August): 177–88. https://doi.org/10.1016/j.fuel.2014.04.052.